



N15

PREPRINT  
IN-02

AVAIL. CASE

© WAIVED

**AIAA 2000-0985**

**Theory and Experiment of Multielement  
Airfoils – A Comparison**

Ryan Czerwiec and J. R. Edwards  
*North Carolina State University, Raleigh, NC*

C. L. Rumsey  
*NASA Langley Research Center, Hampton, VA*

H. A. Hassan  
*North Carolina State University, Raleigh, NC*

**38<sup>th</sup> Aerospace Sciences  
Meeting & Exhibit**  
10-13 January 2000 / Reno, NV

# \*THEORY AND EXPERIMENT OF MULTI-ELEMENT AIRFOILS -- A COMPARISON

Ryan Czerwiec,\* J. R. Edwards†  
North Carolina State University, Raleigh, NC 27695-7910

C. L. Rumsey  
NASA Langley Research Center, Hampton, VA 23681-2199

H. A. Hassan  
North Carolina State University, Raleigh, NC 27695-7910

## Abstract

A detailed comparison of computed and measured pressure distributions, velocity profiles, transition onset, and Reynolds shear stresses for multi-element airfoils is presented. It is shown that the transitional  $k-\zeta$  model, which is implemented into CFL3D, does a good job of predicting pressure distributions, transition onset, and velocity profiles with the exception of velocities in the slat wake region. Considering the fact that the hot wire used was not fine enough to resolve Reynolds stresses in the boundary layer, comparisons of turbulence stresses varied from good to fair. It is suggested that the effects of unsteadiness be thoroughly evaluated before more complicated transition / turbulence models are used. Further, it is concluded that the present work presents a viable and economical method for calculating laminar/transitional/turbulent flows over complex shapes without user interface.

## Introduction

Recent investigation of flows past multi-element airfoils<sup>1,4</sup> indicate that the interaction between the various elements cannot be described by the inviscid equations. Moreover, the results of the calculations are strongly dependent on the selection of transition onset on each of the elements. The work of Ref. 4 represents the first successful attempt at predicting transition onset on multi-element airfoils. In spite of this success, a number of questions remain unanswered. These questions pertain to the

penetration and magnitude of the slat wake deficit at the higher angles of attack.

The true cause of the discrepancy is not known. Three possibilities suggest themselves: three-dimensional effects, adequacy of the two-equation transitional / turbulence model of Ref. 4, and unsteadiness. In order to examine these possibilities, comparison of transition onset and velocity profiles will be carried out for two additional angles of attack,  $\alpha$ , of 16 and 21 degrees. Moreover, comparison with Reynolds stress measurements of McGinley, et al.<sup>5</sup> will be undertaken for selected stations at  $\alpha=8, 16,$  and  $19$  degrees. Wall suction is used to maintain two-dimensional flow in the NASA Langley Low Turbulence Pressure Tunnel (LTPT), and is optimized for  $\alpha=16$  degrees. Thus, special attention will be devoted to this angle of attack.

Pressure distributions, velocity profiles, skin friction, transition onset, and Reynolds stresses<sup>5,9</sup> were measured over a span of five years. The model was reinstalled for each test program. Although care has been taken to maintain the same test configuration, differences in measurements were noted from one test program to the other. Such differences will result in transition occurring at different locations. Experiment indicated that part of the flow, especially in cove regions, was unsteady. This condition would suggest that a time-accurate calculation would be necessary to investigate flows over multi-element airfoils. Because of the incredible computational

---

\*Research Assistant, Mechanical and Aerospace Engineering, Student Member AIAA

†Assistant Professor, Mechanical and Aerospace Engineering, Member AIAA

‡Senior Research Scientist, Fluid Mechanics and Acoustics Division, Senior Member AIAA

§Professor, Mechanical and Aerospace Engineering, Associate Fellow

Copyright © 1999 by the American Institute of Aeronautics and Astronautics, Inc. No copyright is asserted in the United States under Title 17, U. S. Code. The U. S. Government has a royalty-free license to exercise all rights under the copyright claimed herein for Governmental purposes. All other rights are reserved by the copyright owner.

resources required to undertake a time-accurate calculation, one has not been made here. All results were obtained assuming steady conditions. Because of this assumption, the role of unsteadiness will not be addressed in this work.

Ying, et al.<sup>3</sup> compared Reynolds stress calculations with experiment. In this reference, transition onset was assumed using the data of Ref. 9, and the one-equation turbulence model of Spalart and Allmaras<sup>10</sup> was employed. It was indicated in Ref. 3 that eddy viscosity models may not be adequate to reproduce the data in certain regions of the flow. In spite of this potential problem, the model employed in Ref. 4, which is based on the  $k$ - $\zeta$  transitional/turbulence model of Warren and Hassan,<sup>11</sup> will be used here. Considering the fact that we are comparing with different sets of measurements carried out by different people over a five-year span, it is concluded that the model of Ref. 4 does a good job predicting pressure and velocity distributions and transition onset, and a good to fair job predicting the Reynolds stresses.<sup>5</sup>

### Approach

The approach employed in this study is similar to that employed in Ref. 4. In this approach, transitional flows are treated in a turbulence-like manner. The eddy viscosity resulting from the non-turbulent fluctuations,  $\mu_{nt}$ , is dependent on the transition mechanism and can be deduced for low turbulence intensities from linear stability theory. For the present study, transition is a result of Tollmein-Schlichting (T-S) instabilities. The resulting eddy viscosity can be written as<sup>4</sup>

$$\mu_{nt} = C_{\mu} \rho k \tau, \quad C_{\mu} = 0.09 \quad (1)$$

$$\tau = a / \omega \quad (2)$$

$$\frac{\omega v}{q_e^2} = 0.48 \text{Re}_x^{-0.65} \quad (3)$$

$$a = 0.095(Tu - 0.138)^2 + 0.01122 \quad (4)$$

$$Tu = 100 \sqrt{\frac{2}{3} \frac{k_{\infty}}{q_{\infty}^2}} \quad (5)$$

In the above equations,  $\rho$  is the density,  $k$  is the kinetic energy of the fluctuations,  $q$  is the velocity magnitude, and  $Tu$  is the turbulence intensity. Subscripts 'e' and ' $\infty$ ' refer to the edge of the boundary layer and to the freestream, respectively.

With  $\mu_{nt}$  given by Eq. (1) the model of Ref. 4 replaces the turbulent eddy viscosity by

$$(1 - \Gamma)\mu_{nt} + \Gamma\mu_T \quad (6)$$

where  $\Gamma$  is the intermittency and  $\mu_T$  is the turbulent eddy viscosity, which is determined from the  $k$ - $\zeta$  model of Robinson and Hassan.<sup>11</sup> This model is chosen for a number of reasons: it is based on the exact equations for  $k$  and  $\zeta$ , the enstrophy or variance of vorticity; it is free of damping or wall functions; it is coordinate independent, tensorially consistent, and Galilean invariant; it is capable of reproducing the correct growth rates of all free shear layers and suited for the calculation of pressure- or shock-induced separated flows.

The intermittency,  $\Gamma$ , is given by Dhawan and Narasimha<sup>14</sup> and can be expressed as

$$\Gamma = 1 - \exp(-0.412\xi^2) \quad (7)$$

where

$$\xi = \max[s - s_t, 0.0] / \lambda \quad (8)$$

and  $\lambda$  is obtained from the experimental correlation

$$\text{Re}_{\lambda} = 9.0 \text{Re}_{s_t}^{0.75} \quad (9)$$

with  $s_t$  being the location of transition onset, and  $s$  is the distance along the surface, measured from the stagnation point. In general,  $s_t$  can be the point where turbulent spots first appear, or where skin friction, heat transfer, or recovery factor is a minimum, or when

$$R_T = \frac{1}{C_{\mu}} \frac{v_{nt}}{v} = 1.0. \quad (10)$$

Equation (10) was used in Ref. 4 to determine transition onset. Although Eq. (10) does not correlate directly with any of the characteristics of the hot film signals that were used to determine transition onset in experiments,<sup>9</sup> onset predictions were in good agreement with the measurements of Ref. 9. The only exception was transition onset on the slat at  $\alpha=8$  degrees, for which predicted transition onset did not agree with experiment. Nonetheless, reasonably good agreement with velocity measurements downstream of  $x/c = .85$  was indicated in Ref. 4 when Eq. (10) was used.

The present model was incorporated into CFL3D.<sup>13</sup> CFL3D is a widely used code, and a number of previous investigators used the code to study a variety of problems, including multi-element airfoils. In addition to incorporating the  $k$ - $\zeta$  transitional / turbulence model, the time derivative preconditioning scheme of Edwards and Thomas<sup>15</sup> is now a permanent feature of CFL3D. All the results presented here make use of the preconditioned code.

## Results and Discussion

The results presented here are for the McDonnell Douglas 30P-30N landing configuration for angles of attack of 8, 16, 19, and 21 degrees, freestream Mach number,  $M_\infty$ , of 0.2, and a chord Reynolds number of 9 million. Pressure distributions, velocity profiles, and transition predictions are presented for all angles of attack, and Reynolds shear stresses are presented for all but the 21 degrees angle of attack. The tunnel's turbulence intensity,  $Tu$ , is chosen as 0.05.

In order to facilitate comparison with previous results, the four-zone free air grid used in Refs. 2-4 is used in the present calculations. It is assumed that the gaps and overhangs of the slat and flap remained constant during repeated model installations.

### 1. $\alpha=16$ Degrees Comparisons

As indicated earlier, tunnel wall suction was employed for this angle of attack in order to approximate two-dimensional flow. Figure 1 compares computed pressure distributions with experiment. As is seen in the figure, the pressure distributions are accurately reproduced. The loading on the slat and main airfoil are much higher than the  $\alpha=8$  degrees results and are roughly along a linear variation between the  $\alpha=8$  degrees and  $\alpha=19$  degrees cases described in Ref. 4.

Transition prediction for all elements is given in Fig. 2. As was noted in Ref. 4, no attempts were made to probe the cove regions and the aft portion of

the flap. The circles in the figure indicate the start and end (when indicated) of measured transition, the squares indicate computed onset prediction, and the crosses indicate where the computed values of the intermittency reach 1/2. In general, good agreement with experiment is indicated, and the results are not much different from those at  $\alpha=19$  degrees. It is to be noted that the maximum value of  $\mu_T / \mu_\infty$  in the region below the main airfoil is less than 100. Thus, the apparent disagreement with experiment on the lower surface of the main airfoil is not as severe as it appears.

Figure 3 shows the stations at which profiles of velocity and Reynolds stresses are compared with experiment. Data is not available at all stations for each angle of attack. Thus results will be shown only for stations for which experimental data is available. Figure 4 displays the velocity profiles at eight stations on the main airfoil and flap. As is seen in the figure, the penetration of the main airfoil wake is well-captured. Departures in the penetration and magnitude of the slat wake deficit are noted in the figure. The maximum error is less than 3%, compared to about 5% for  $\alpha=19$  degrees. This number represents the difference between peak measured and calculated values divided by peak measured value. Because the tunnel wall suction was optimized at  $\alpha = 16$  degree to achieve as 2-D a flow as possible, it appears that 3-D effects play a minor role in this case and are probably not the cause of the discrepancy in the slat wake. Thus, the cause of the discrepancy is, in all probability, unsteadiness or a limitation of the present model. The quantity  $d/c$  appearing in the figure is the ratio of the surface-normal distance to the wing chord length.

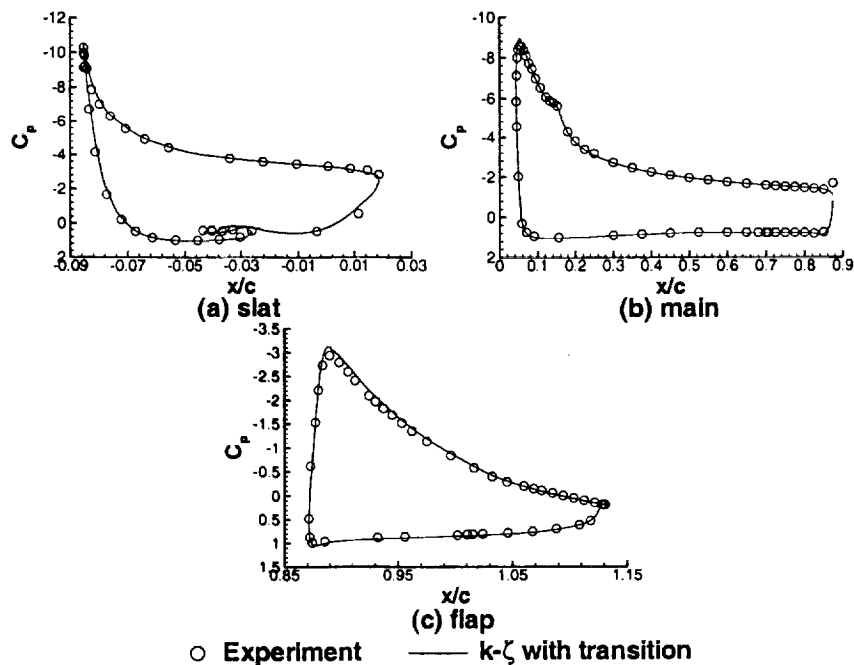


Figure 1: Pressure distribution for  $\alpha = 16$  degrees

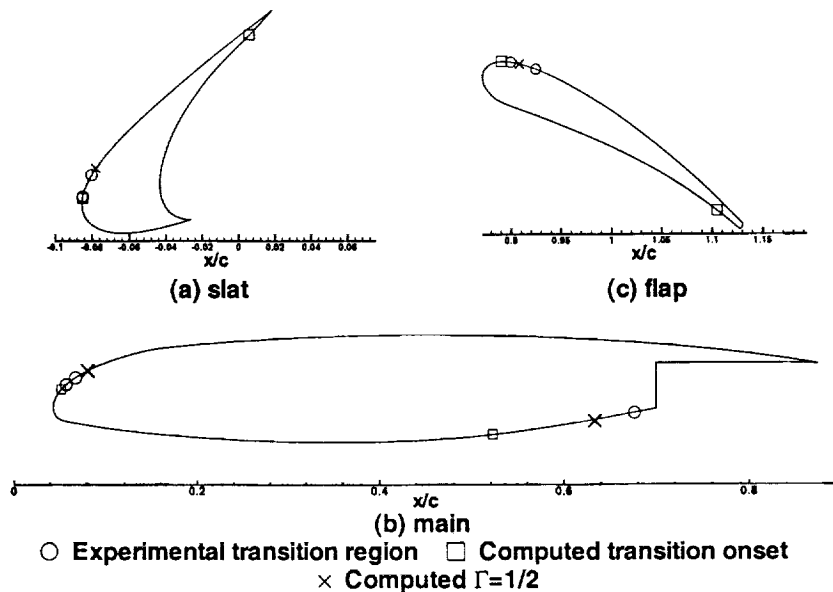


Figure 2: Transition locations for  $\alpha=16$  degrees

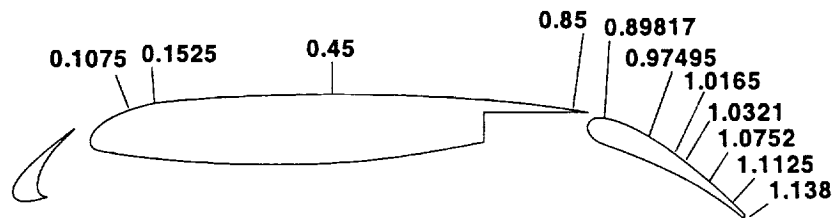


Figure 3: Surface-normal profile  $x/c$  stations

Figure 5 compares Reynolds shear stresses in streamline coordinates at four stations. It was suggested in Ref. 5 that there were differences between Phase 1 and Phase 2 measurements of the Reynolds stresses. They were carried out a year apart. This necessitated removal and reinstallation of the model. Moreover, emphasis was placed on studying wake regions. This resulted in using a hot wire whose size is not suited for resolving the boundary layer region. Measurements were further complicated by the unsteadiness of the flow, especially in the cove regions. As may be seen from Fig. 5, the stations immediately ahead and immediately behind the flap gap are not as well predicted as stations away from the gap. This may be a result of the unsteadiness in the cove of the main element or, a result of a slight change in the size of the flap gap. It was indicated in Ref. 3, that slight

changes in the flap gap have an important influence on the flow in that region.

## 2. $\alpha=21$ Degrees Comparisons

For this angle of attack, comparisons will be made for pressure distribution, transition onset, and velocity measurements. Although turbulent stresses are calculated as part of the solution, no experimental data is available for comparison. Experiment indicates that the flow at this angle, which is near the stall region, is rather unsteady. Thus, it is expected that unsteadiness will have a major influence in this case.

Figure 6 compares the calculated pressure distribution with experiment. Again, excellent agreement is indicated. Figure 7, which compares transition onset predictions with experiment, shows the same level of good agreement as for  $\alpha=16$  and 19 degrees. As seen in Fig. 8, which

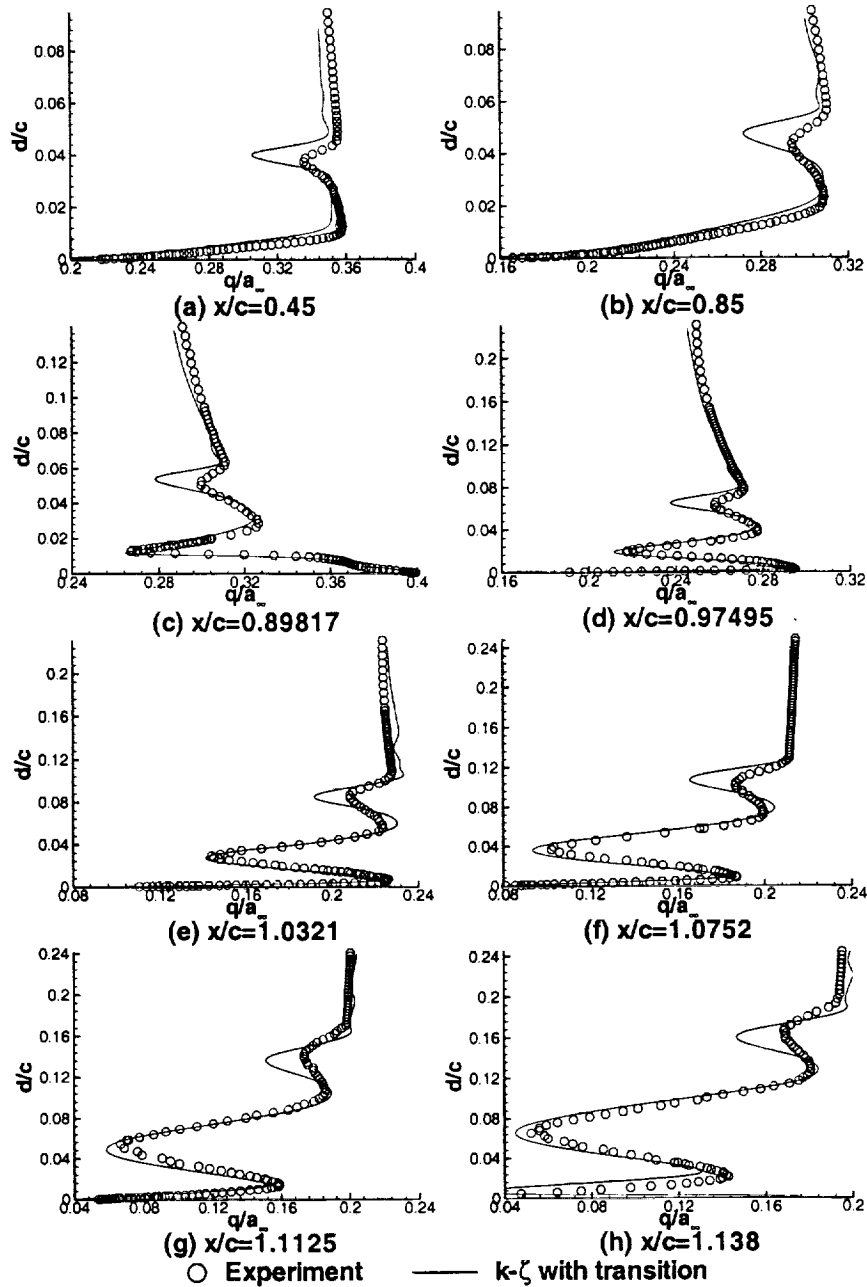


Figure 4: Velocity profiles for  $\alpha=16$  degrees

compares calculated velocities with experiment over the two main airfoil stations and five flap stations that, with the exception of the slat wake region, the agreement is as good as for the other angles of attack. Note that 9000 cycles were run to obtain the results, which is the same number for all the other angles of attack. Both  $C_\ell$  and  $C_d$  were converged at 6,000 cycles and no change was observed after 9,000 cycles. However, a limit cycle developed in the residual convergence history after the residual was

reduced by  $3\frac{1}{2}$  orders of magnitude. This limit cycle is a result of oscillations in the cove regions. Thus, true convergence was not reached here, and the oscillations near the slat wake in the numerical solution are clearly a non-physical result. This case was the subject of detailed investigation in Ref. 3. It was indicated there that oscillations obtained when a steady state solution was attempted prevented convergence. On the other hand, a time-accurate computation did not show evidence of gross unsteadiness. The results of Ref. 3 clearly illustrate the importance of accounting for unsteadiness in the flow.

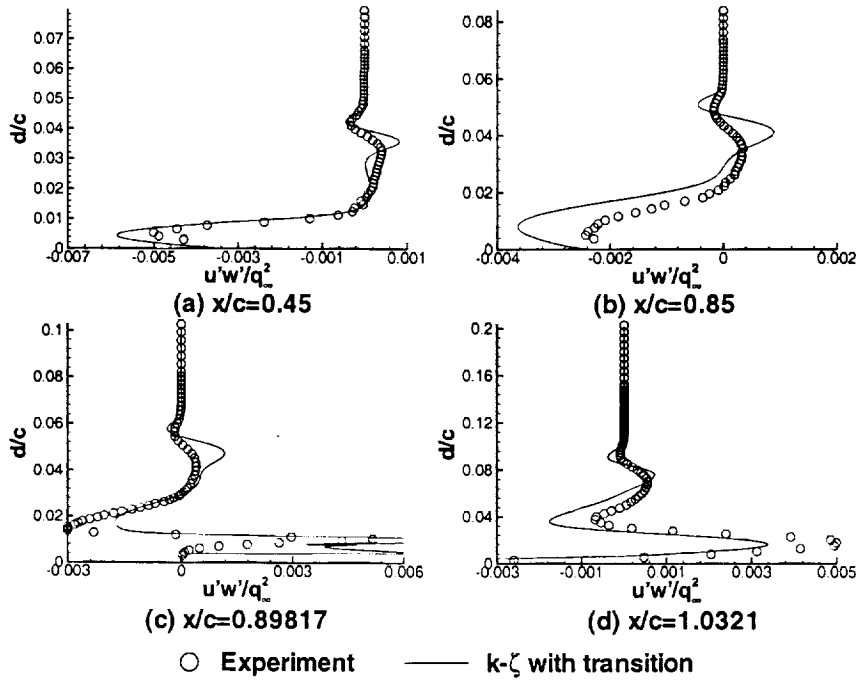


Figure 5: Streamwise Reynolds stress for  $\alpha=16$  degrees

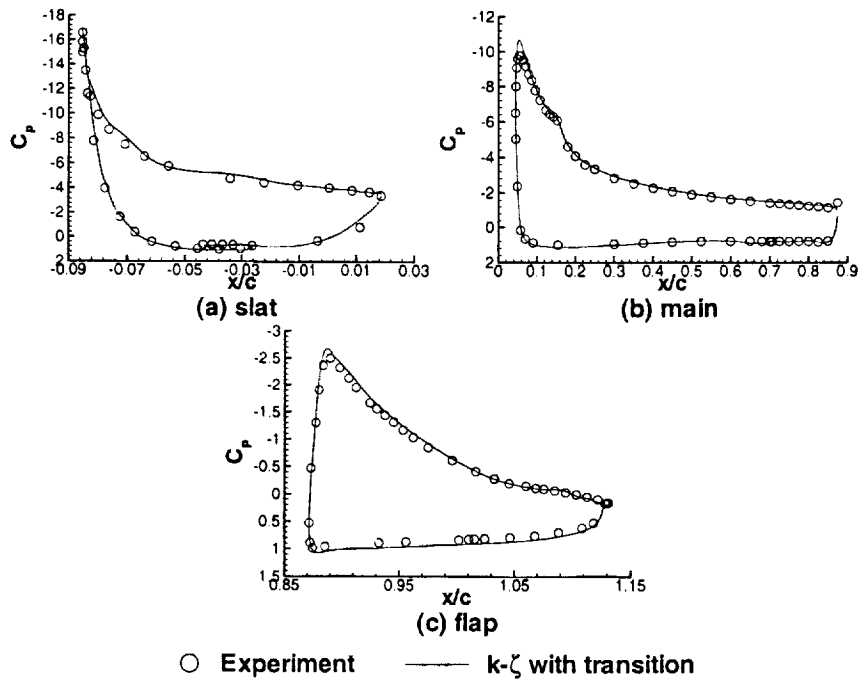


Figure 6: Pressure distribution for  $\alpha=21$  degrees

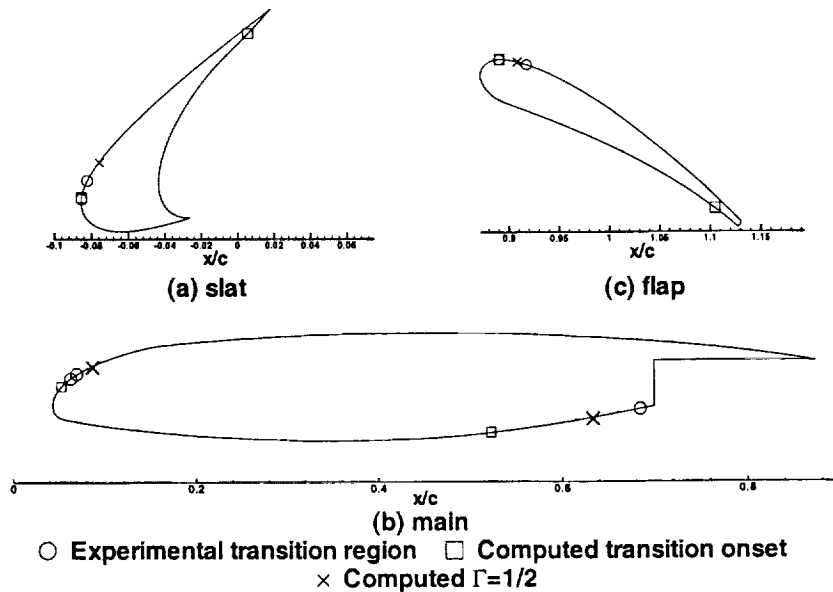


Figure 7: Transition locations for  $\alpha=21$  degrees

### 3. $\alpha=8, 19$ Degrees Comparisons

Comparisons at  $\alpha = 8$  and  $19$  degrees involving pressure distributions, transition onset, and velocities are given in Ref. 4. Thus, only Reynolds shear stress results will be examined here.

Figures 9 and 10 compare Reynolds shear stress for  $\alpha=8$  and  $19$  degrees, respectively. In general, the agreement is similar to those for  $\alpha = 16$  degree case. The results for  $\alpha = 19$  were the subject of detailed investigation in Ref. 3. It was suggested there that the discrepancy at the  $x/c = .89817$  is a result of using an eddy viscosity model. The implication there is that a stress model would be necessary to explain noted differences. This can be a possible cause of the discrepancy. However, since a nonlinear stress model was not used in this work, we are in no position to make a definitive statement on this issue.

#### Concluding Remarks

It is shown here that the present model does a good job predicting pressure distribution, velocity profiles, transition onset and Reynolds stresses on multielement airfoils. The only exceptions are the profiles in the slat wake, whose depth tends to be overpredicted in general. The predicted slat wake profiles for  $\alpha=21$  degrees are particularly poor. Not only is the wake depth overpredicted, but oscillatory behavior is also evident above the wake itself. This angle of attack required a time-accurate calculation in Ref. 3 in order to obtain a physically

meaningful solution. This suggests that the oscillations in this case may be a result of attempting to model unsteadiness with a steady-state algorithm.

The role of unsteadiness remains a major unknown. It appears that its role must be understood before one attempts more sophisticated transitional / turbulence modeling. Experiments have noted that the flow for most of the angles of attack is unsteady. Even when one carries out a steady calculation, the flow in the cove regions remains oscillatory, which can have a major influence on the results. This suggests that a combination of time accurate calculations and nonintrusive measurements is required to explain and predict the flow in the slat wake region.

Finally, this work demonstrates the ability to calculate laminar, transitional, and turbulent flow routinely, without user interface, and at a reasonable cost.

#### Acknowledgements

This work is supported in part by NASA grant NAG-1-1991. Part of the computation was carried out at the North Carolina Supercomputing Center and at NAS. The authors would like to express their appreciation to Cathy McGinley of NASA Langley Research Center for providing us with the Reynolds stress data and for many helpful discussions and to Dr. S. Rogers of NASA Ames Research Center for the use of data reduction software. Further, the authors would like to acknowledge many helpful discussions with Dr. N. Chokani of North Carolina State University.



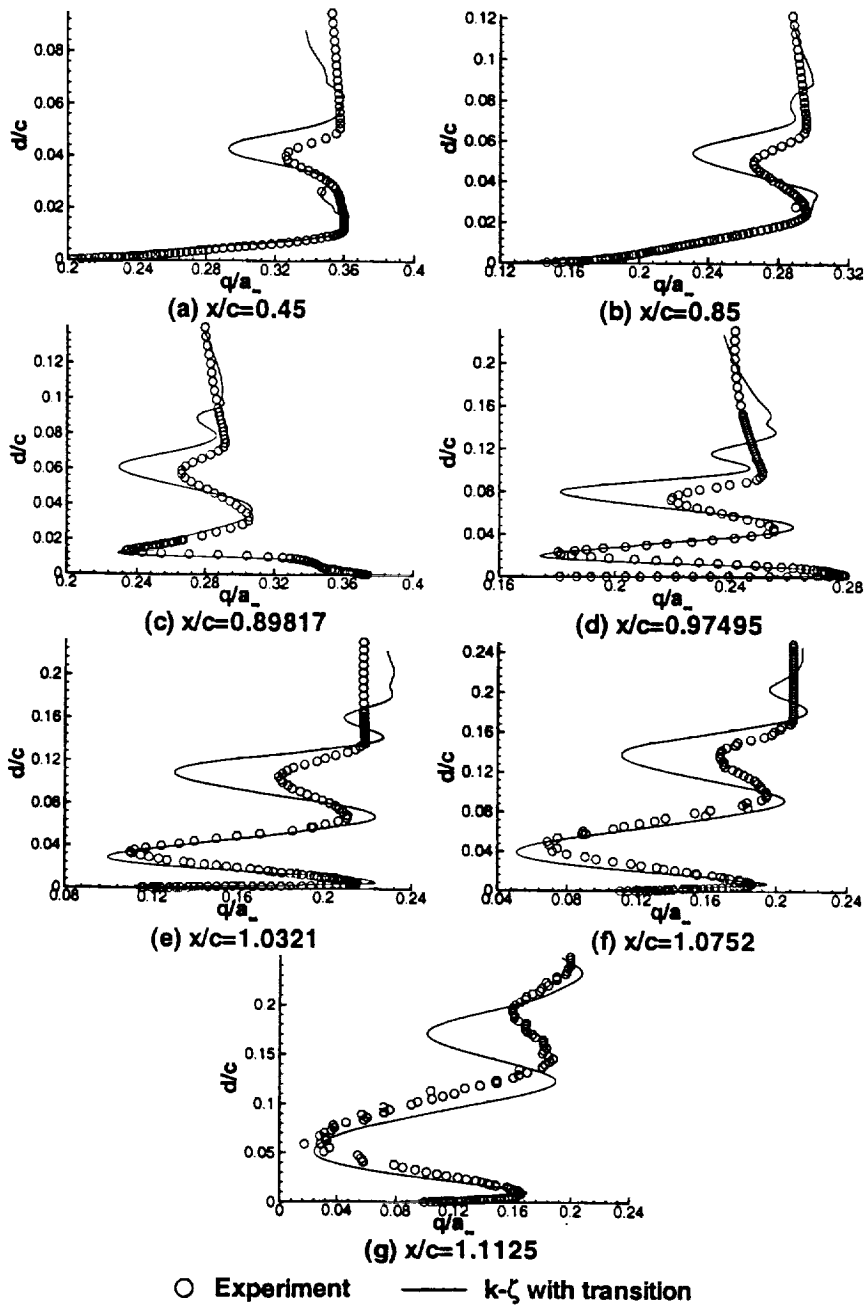


Figure 8: Velocity profiles for  $\alpha=21$  degrees

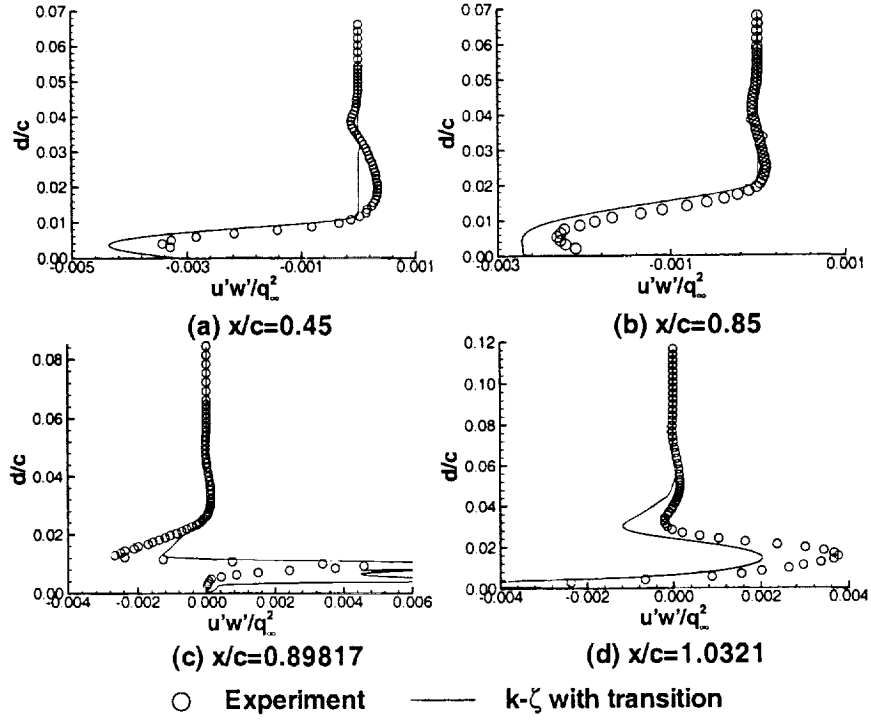


Figure 9: Streamwise Reynolds stress for  $\alpha=8$  degrees

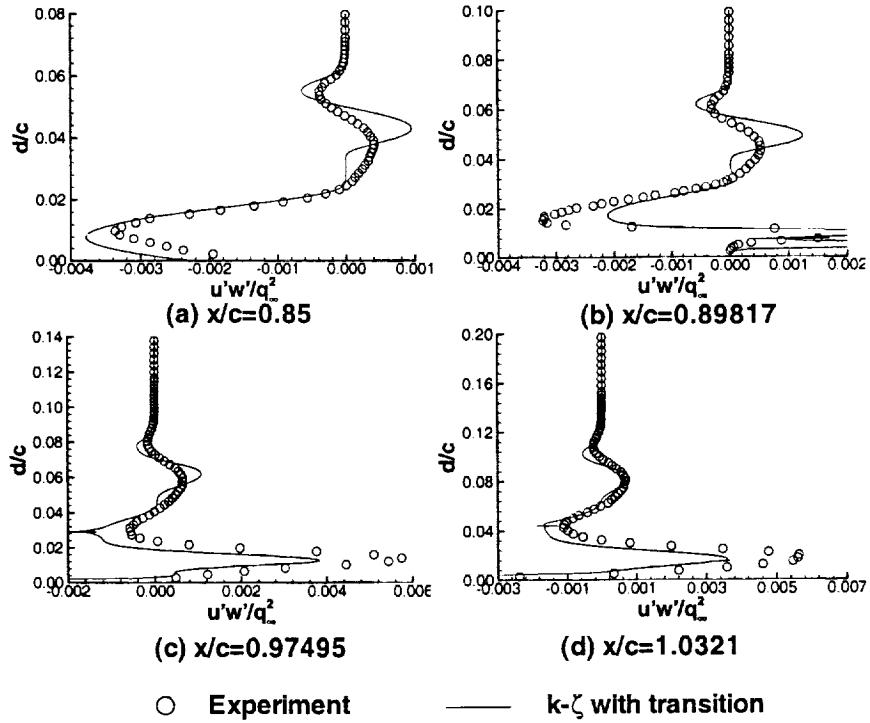


Figure 10: Streamwise Reynolds stress for  $\alpha=19$  degrees

### References

1. Lynch, F. T., Potter, R. C. and Spaid, F. W., "Requirements for Effective High-Lift CFD," Proceedings, 20th ICAS Congress, September 1996.
2. Rumsey, C. L., Gatski, T. B., Ying, S. X., and Bertelrud, A., "Prediction of High-Lift Flows Using Turbulent Closure Models," *AIAA Journal*, Vol. 36, No. 5, May 1998, pp. 765-744.
3. Ying, S. X., Spaid, F. W., McGinley, C. B., and Rumsey, C. L., "Investigation of Confluent Boundary Layers in High-Lift Flows," *Journal of Aircraft*, Vol. 36, No. 3, May-June 1999, pp. 550-562.
4. Czerwiec, R. M., Edwards, J. R., Rumsey, C. L., Bertelrud, A. and Hassan, H. A., "Study of High-Lift Configurations Using  $k$ - $\zeta$  Transition / Turbulence Model," AIAA Paper 99-3186, June 1999.
5. McGinley, C. B., Anders, J. B., and Spaid, F. W., "Measurement of Reynolds Stress Profiles on a High-Lift Airfoil," AIAA Paper 98-2620, June 1998.
6. Chin, V. D., Peters, D. W., Spaid, F. W., and McGhee, R. J., "Flowfield Measurements About a Multi-Element Airfoil at High Reynolds Numbers," AIAA Paper 93-3137, July 1993.
7. Klansmeyer, S. M. and Lin, J. C., "An Experimental Investigation of Skin Friction on a Multi-Element Airfoil," AIAA Paper 94-1870, June 1994.
8. Spaid, F. W., and Lynch, F. T., "High Reynolds Number Multi-Element Airfoil Flowfield Measurements," AIAA Paper 96-0682, January 1996.
9. Bertelrud, A., "Transition on a Three-Element High Lift Configuration at High Reynolds Numbers," AIAA Paper 98-0703, January 1998.
10. Spalart, P. R. and Allmaras, S. R., "A One-Equation Turbulence Model for Aerodynamic Flows," AIAA Paper 92-0439, January 1992.
11. Warren, E. S. and Hassan, H. A., "A Transition Closure Model for Predicting Transition Onset," *Journal of Aircraft*, Vol. 35, No. 5, September-October 1998, pp. 769-775.
12. Robinson, D. F. and Hassan, H. A., "Further Development of the  $k$ - $\zeta$  (Enstrophy) Turbulence Closure Model," *AIAA Journal*, Vol. 36, No. 10, October 1998, pp. 1825-1833.
13. Krist, S. L., Biedron, R. T. and Rumsey, C. L., *CFL3D User's Manual (Version 5.0), Second Edition*, NASA Langley Research Center, Hampton, VA, September 1997.
14. Dhawan, S. and Narasimha, R., "Some Properties of Boundary Layer Flow During Transition from Laminar to Turbulent Motion," *Journal of Fluid Mechanics*, Vol. 3, No. 4, 1958, pp. 414-436.
15. Edwards, J. R. and Thomas, J. L., "Development and Investigation of  $O(Nm^3)$  Preconditioned Multigrid Solvers for the Euler and Navier-Stokes Equations" AIAA Paper 99-3263, June 1999.